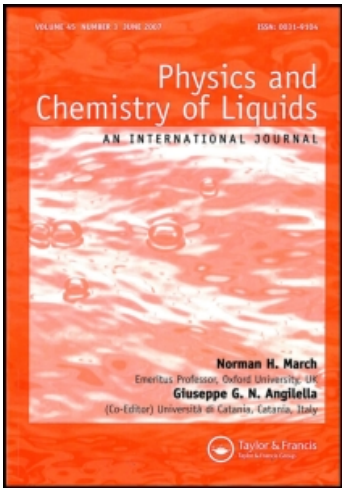

Physics and Chemistry of Liquids
Publication details, including instructions for authors and subscription information:
http://www.informaworld.com/smpp/title~content=t713646857

Visualization of Shear-Induced Ordering in Atomic Liquids

W. C. Sandberg[a]; Upul Obeysekare[b]; Chas Williams[b]; Aron Qasba[b]
[a] Laboratory for Computational Physics and Fluid Dynamics, Naval Research Laboratory, Washington, D.C. [b] Naval Research Laboratory, Center for Computational Science, Washington, D.C.

To cite this Article Sandberg, W. C. , Obeysekare, Upul , Williams, Chas and Qasba, Aron(1997) 'Visualization of Shear-Induced Ordering in Atomic Liquids', Physics and Chemistry of Liquids, 35: 2, 67 — 80
To link to this Article: DOI: 10.1080/00319109708030574
URL: http://dx.doi.org/10.1080/00319109708030574

Phys. Chem. Liq., 1997, Vol. 35, pp. 67–80
Reprints available directly from the publisher
Photocopying permitted by license only

VISUALIZATION OF SHEAR-INDUCED ORDERING IN ATOMIC LIQUIDS

W.C. SANDBERG,[a] UPUL OBEYSEKARE,[b] CHAS WILLIAMS[b] and ARON QASBA[b]

[a]*Laboratory for Computational Physics and Fluid Dynamics, Naval Research Laboratory, Washington, D.C. 20375-5344;*
[b]*Center for Computational Science, Naval Research Laboratory, Washington, D.C. 20375–5344*

(Received 23 December 1996)

A visualizaton and animation capability has been extended to provide insights into the short time dynamics in atomic liquids. Non-Equilibrium Molecular Dynamics shear flow simulations have been carried out in several isotopically substituted Lennard-Jones liquids for four shear rates. The results of these simulations have been visualized and animated to show the computed trajectories of selected atoms and the variation in their local environment in a sheared systems. Linear ordering along the direction of shear is seen at the highest shear rate. This ordered structure is inclined in the plane normal to the shear direction. The local environments about chosen atoms are observed to undergo extensive deviation from a spherical shape.

Keywords: Visualization; animation; shear-induced order; NEMD

1. INTRODUCTION

Fluctuations about thermal equilibrium in atomic liquids result in single particle motions which are well characterized by the velocity autocorrelation function (VACF), mean square displacement and the corresponding self-diffusion coefficients. In dense liquids, the negative region of the VACF indicates that there is on average significant backscattering of a typical atom from its first coordination shell (which has been often considered to be cage-like at short times). The extent to which the local environment is or is not cage-like has not been extensively studied. Yet it is the dynamics of the local

environment which is responsible for the short-time dynamics manifested in the velocity autocorrelation function. An investigation of the local environment is therefore of interest. It is now well-known that the imposition of a shear velocity profile can dramatically alter transport dynamics and the structural arrangement in liquids. The nature of the relationship of the structural rearrangement to the altered transport behavior is however, still largely unknown. NEMD simulations of Lennard-Jones liquids, [1], did reveal that diffusion anisotropy and local structural reordering accompany the onset of non-Newtonian flow. It was also found that unconvected diffusion is enhanced especially along the flow direction with increasing shear rate.

In a study of the self-diffusion coefficients for liquid mixtures in a shear flow [2], it was observed that each of the three diagonal elements of the self-diffusion tensor $D_{\alpha\alpha}$, where the self-diffusion coefficient for the impurity atom, $\underline{D}$, is given by the Green-Kubo expression,

$$D_A = 1/3 \int_0^\infty < V_i(0) \cdot V_i(t) > dt, \tag{1}$$

increase initially with shear rate, reach a maximum (which depends on the mass of the solute particle, m_A) and then decreases. At the higher shear rates the suppression of the D_{yy} and D_{zz} elements of the self-diffusion tensor and enhancement of D_{xx} along the flow direction certainly suggested structural rearrangement. A functional relationship was found between the variations in the diagonal elements of the self-diffusion tensor, the ratio of mixture masses, and the strength of the applied shear field. It is the intent of the current work to carry out 3-D visualization of the local structure associated with these sheared systems to assist in elucidating how the local structural dynamics vary with the field strength and hence to gain insight into the collective origins of shear-induced anisotropy in self-diffusion.

2. THEORY AND SIMULATION METHOD

In order to begin to augment our understanding to how the local structural dynamics may lead to the observed behaviour of the self-diffusion tensor components in a shear flow, we have carried out

several simulations and visualized those results. The equilibrium (zero shear) configuration and the computational orientation of the sheared system are shown in Figures 1 and 2 respectively.

Simulations were carried out for four impurity/host atomic mass ratios: $m^* = m_A/m_B$ of 0.5, 1.0, 2.1, and 3.3 corresponding to the mass ratios for neon, argon, krypton, and xenon respectively in argon. The simulations were performed on a unit cell of volume V containing 256 atoms with an interaction potential

$$\phi(r) = 4\epsilon((\sigma/r)^{12} - (\sigma/r)^6), \tag{2}$$

with the potential parameters of argon used for all simulations. The interaction was truncated at 2.5σ. LJ reduced units were used;

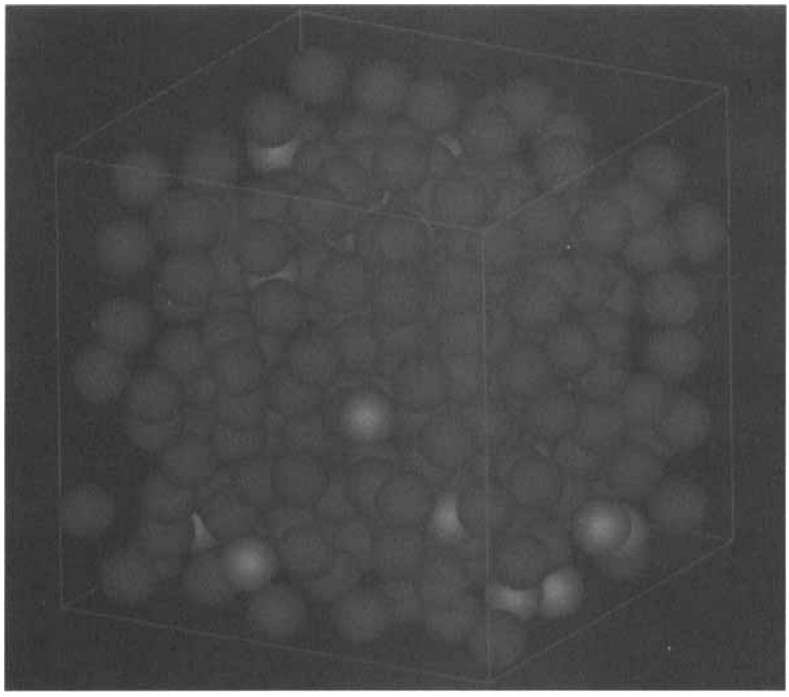

FIGURE 1 Equilibrium configuration of Lennard-Jones liquid mixture. Red represents dilute (approximately ten percent of the total number of atoms) component atoms. See Color Plate I.

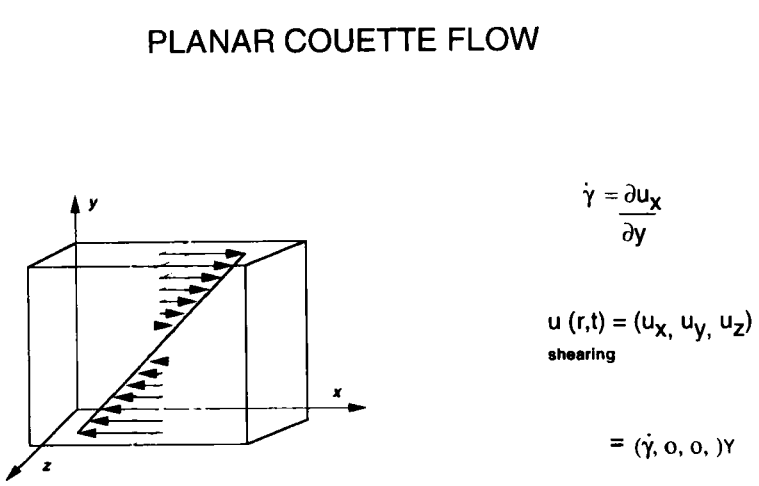

FIGURE 2 Shear flow orientation in the fundamental computational cell.

$\rho^* = N\sigma^3/V$, and $T^* = k_B T/\epsilon$. The simulation is in reduced time units,

$$t^* = t(\epsilon/m(\sigma)^2)^{1/2}, \tag{3}$$

with a magnitude of 0.015. The reduced shear strain rate is given by

$$\dot{\gamma}^* = \dot{\gamma}(\sigma^2 m/\epsilon)^{1/2}. \tag{4}$$

Each simulation was equilibrated for 2000 times steps at the desired temperature. Zero shear rate simulations were run, following thermal equilibration, at constant energy for 20 000 steps. Shear simulations were run for five reduced shear strain rates: 0.5, 1.0, 1.5, 2.0 and 3.0, at the state point specified by $\rho^* = 0.844$ and $T^* = 0.722$.

The SLLOD algorithm was used to impose planar Couette flow on the system [3,4]. We take the streaming velocity to be in the x-direction and the linear velocity gradient,

$$du_x/dy = \dot{\gamma}, \tag{5}$$

is established in the y-direction, where $\dot{\gamma}$ is the magnitude of the imposed strain rate. The peculiar or thermal momentum is denoted by

$\tilde{\mathbf{p}}$. For atomic positions, denoted by $\mathbf{R}$, we have

$$\dot{\mathbf{R}}_i = p_i/m + \mathbf{R}_i \cdot \nabla \mathbf{p}_i, \tag{6}$$

$$\dot{\mathbf{p}}_i = \mathbf{F}_i - \mathbf{p}_i \cdot \nabla \mathbf{p}_i/m - \beta \mathbf{p}_i, \tag{7}$$

where

$$\beta = \sum_{i=1}^{N} (\mathbf{p}_i \cdot \mathbf{F}_i - \mathbf{p}_i \mathbf{p}_i : \nabla \mathbf{p}_i/\mathbf{m}) / \sum_{i=1}^{N} \mathbf{p}_i \cdot \mathbf{p}_i. \tag{7a}$$

For the Couette flow chosen this becomes,

$$\dot{R}_x = p_x/m = (\tilde{p}_x/m) + \dot{\gamma} R_y/m, \tag{8}$$

$$\dot{R}_y = p_y/m = \tilde{p}_y/m, \tag{9}$$

$$\dot{R}_z = p_z/m = \tilde{p}_z/m, \tag{10}$$

$$\dot{\tilde{p}}_x = F_x - \dot{\gamma} \tilde{p}_y - \beta \tilde{p}_x, \tag{11}$$

$$\dot{\tilde{p}}_y = F_y - \beta \tilde{p}_y, \tag{12}$$

$$\dot{\tilde{p}}_z = F_z - \beta \tilde{p}_z, \tag{13}$$

where the α component of the force on an atom is F_α, the momentum is p_α, the peculiar momentum is $\tilde{p}_\alpha$, (i.e., that component of the momentum in excess of the streaming flow momentum), and β is the Gaussian isokinetic thermostat coefficient. We employ in the NEMD computations a combination of Lees-Edwards [5], (in the y-direction), and periodic, (in the x and z directions), boundary conditions.

We computed the mean sqaure displacement, namely,

$$[r_A(t)]^2 = 1/NA \sum_{i=1}^{NA} [\mathbf{R}'_i(t) - \mathbf{R}'_i(0)]^2, \tag{14}$$

where the atom positions, $\mathbf{R}'_i$, are the absolute positions which have not been operated on by the periodic boundary conditions.

3. RESULTS AND DISCUSSION

The Application Visualization System (AVS) is commercial software whose general application to molecular dynamics has been described earlier [6], and coupled to Virtual Reality (VR) technology for visualizing complex dynamic processes [7]. AVS uses a flexible visual programming environment that allows one to construct custom visualization applications. We report here on several extensions made to AVS which are applicable to the analysis of Non-Equilibrium Molecular Dynamics (NEMD) investigations. We have developed a suite of specialized modules for visualizing time-dependent data from molecular dynamics simulations and have incorporated these modules into AVS. This suite includes data readers from common file formats such as MacAtom, filtering modules such as depicting a spherical sub-domain within the computational volume, and modules for displaying the trajectory of a selected atom, along with its' changing environment, over a period of time-steps. An example of a typical network of modules constructed for use in this work is shown in Figure 3. This network loads MD datasets from either a binary file format (DFMD) using the National Center for Supercomputing Application's Hierarchical Data Format (HDF) or from a Macintosh MacAtom data file and displays them using the Scatter Dots and Geometry Viewer modules.

In the visualizations carried out for the present work we selected an arbitrary atom of the dilute species (type *A*) and those atoms (of species *A* or *B* or both) which are located in a spherical shell, corresponding to the first coordination shell, drawn about this atom. The arbitrary atom selected was chosen from those which were a diameter or more away from either the center of the box or the top or bottom boundary. Choosing atoms away from the top or bottom boundary was done to enhance the observation interval by reducing the number of exits and re-entrys associated with the periodic boundary conditions. Initially this was not done and the atoms were chosen randomly. The resulting animations of trajectories were

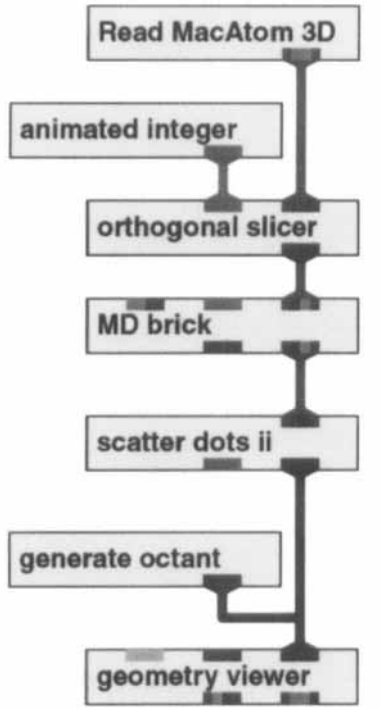

FIGURE 3 AVS Networks to load MD datasets using the **Read MacAtom 3D** module and generate local neighborhood and trajectory of selected atom. See Color Plate II.

difficult to interpret as atoms were frequently exiting and re-entering the box and thus disrupting continuity of the trajectories. Atoms were also chosen away from the center of the simulation cell. Atoms selected from the vicinity of the plane of zero shear of the cell were observed to spend most of the time fluctuating locally about that plane, as in a thermal equilibrium simulation. Occasionally a large velocity fluctuation would displace an atom into a region of higher horizontal velocity and then it would move away under the action of the applied shear field. However, much of the time central atoms are uninteresting. A typical subset of atoms selected for observation is show in Figure 4.

Observations of the spatial configuration of the selected atoms at specific time intervals is of interest and can be visualized using any number of available software packages. We thought it might be

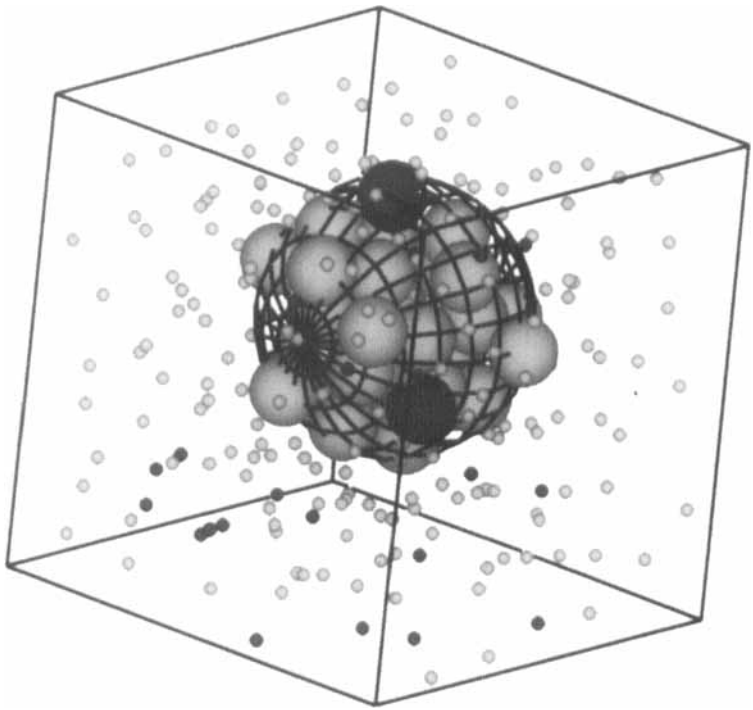

FIGURE 4 Spherical sub-domain selected from the total simulation cell. See Color Plate III.

considerably more informative to also observe the trajectories of the selected atoms as the simulation proceeds. For this purpose several new modules were written and incorporated into AVS. A trajectory module, Scatter Trajec, was written to extract coordinates for a given atom or atoms during a specified time range. The trajectory can then be displayed as a set of continuous spheres indicating all the previous positions of the specified atom up to its' current position, in its' current local environment. One of course saves the previous local environments corresponding to the previous selected atom positions and velocities so that the time history of the characteristics of the local environment may also be investigated. After several traverses of the domain the trajectory can become quite complex. Interpretation is made easier by color coding the temporal sequence of the path. That is, one can move through an arbitrary sequence of colors as the

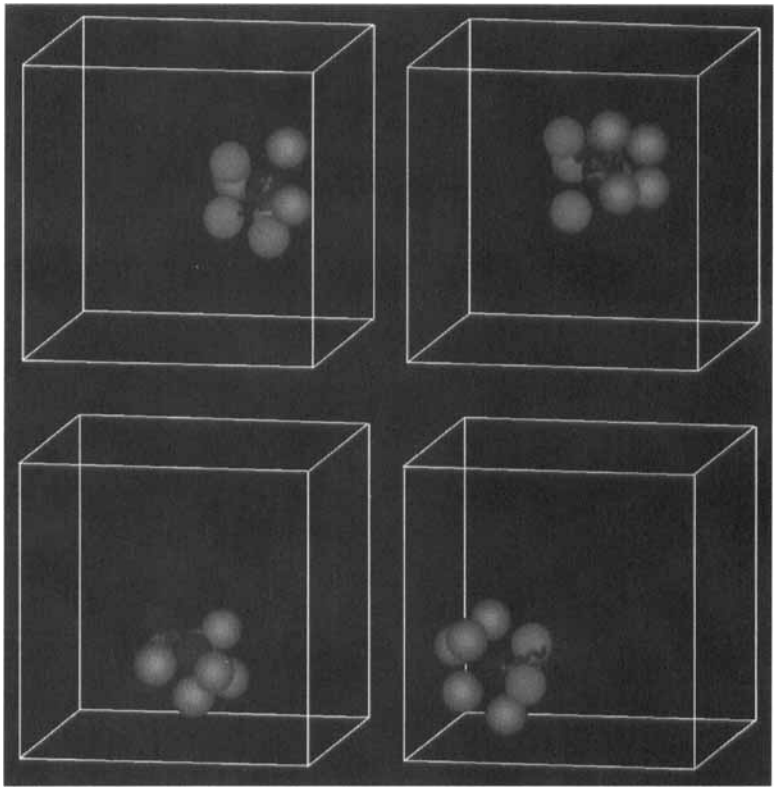

FIGURE 5 Evolution of the trajectory of selected atom and the configuration of its' local environment at time steps 20250, 20500, 20750 and 21,000 in thermal equilibrium. See Color Plate IV.

trajectory evolves. We chose to indicate the starting location by violet and move progressively to blue, orange, and finally red to represent the ending point of a trajectory. Trajectories for a selected atom of reduced mass $m^* = 0.5$ within its' variable and deforming environment are presented in Figures 5, 6, 7 and 8 for four reduced shear rates, $\gamma^* = 0,1,2,3$ respectively. Each of the four trajectories of the selected atom are shown including the instantaneous configuration of its neighbors at the time step indicated. The trajectories shown are from time step 20 001 up to time steps 20 250, 20 500, 20 750, and 21 000 respectively. The atoms themselves are also color coded to keep track of the variations in local environment from the initial configuration.

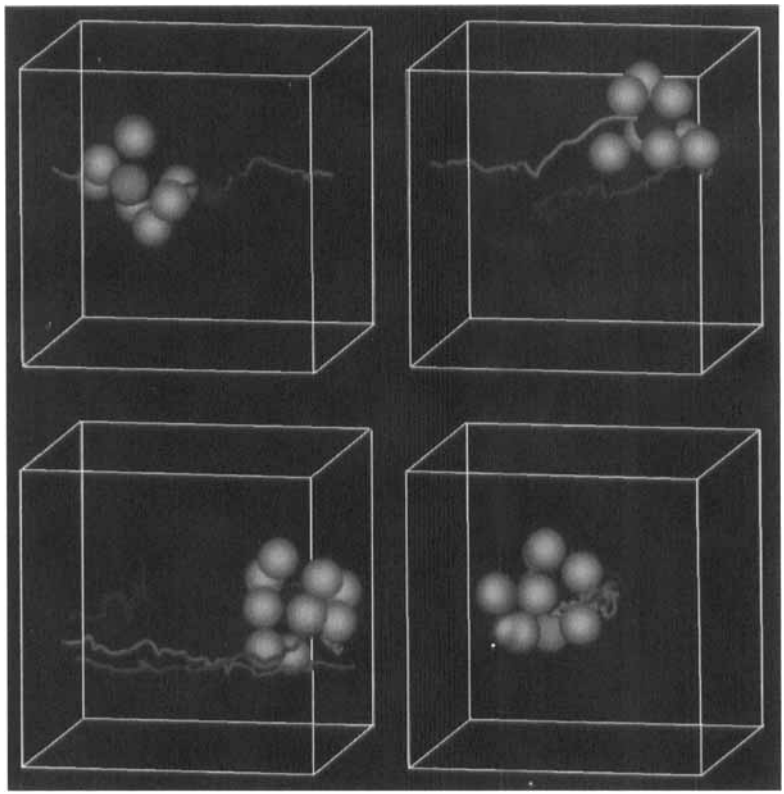

FIGURE 6 Evolution of the trajectory of a selected atom and the configuration of its' local environment at time steps 20250, 20500, 20750 and 21,000 at a reduced shear rate $\dot{\gamma}^* = 1$. See Color Plate V.

The central atom at time step 20 001 is indicated by blue. The 1st shell neighbors at time step 20 001 are green and new first shell neighbors which subsequently enter the shell are red. Additional impurity or dilute species atoms which enter the shell are also blue. One notices in these visualizations that the local environment seldom appears to be spherically symmetric and can take on quite distorted shapes. This suggests that the use of the static term 'cage' is insufficient to accurately describe dynamic variations in complex local environments in dense liquids. An extension of this work has led to the development of unstructured grid-based techniques for the quantitative analysis of

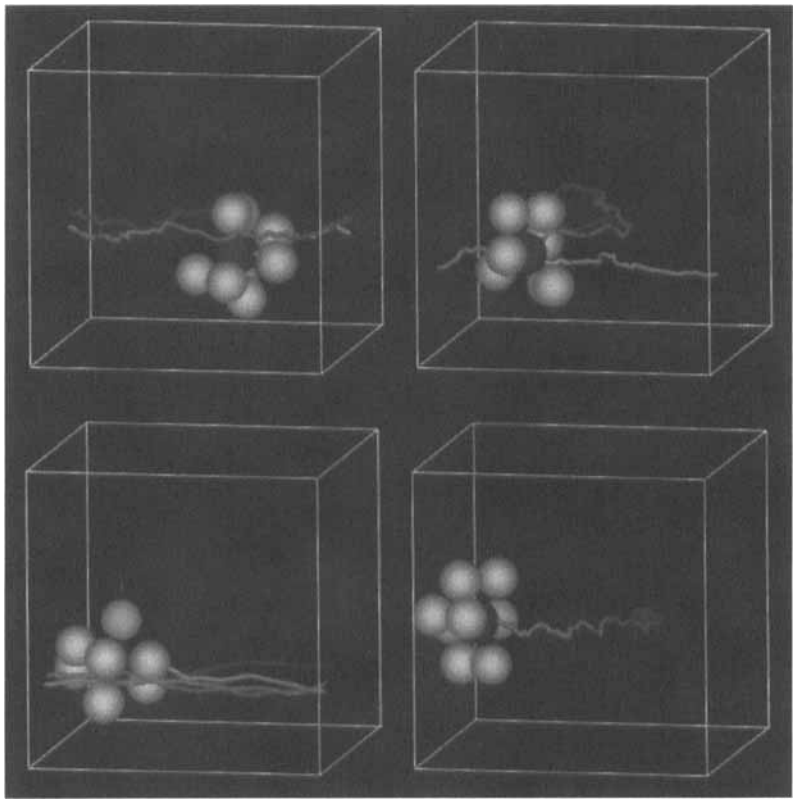

FIGURE 7 Evolution of the trajectory of a selected atom and the configuration of its' local environment at time steps 20250, 20500, 20750 and 21,000 at a reduced shear rate $\dot{\gamma}^* = 2$. See Color Plate VI.

the time-varying accessible surface area and excluded volume of the local environment in these sheared liquid systems. Those results will be reported separately .

It can be also seen that, as the shear rate increases, considerably more traversals of the box occur and the trajectories are quite restricted in the direction normal to the flow direction. This confinement appears to be essentially planar at the highest shear rate. To examine this further, additional modules were written for AVS to allow for two perpendicular views of all the atoms. The first of these views is shown in Figure 9 which is a view looking from the side of the box. that is in the x-y plane, which is the plane of shear. The atoms in

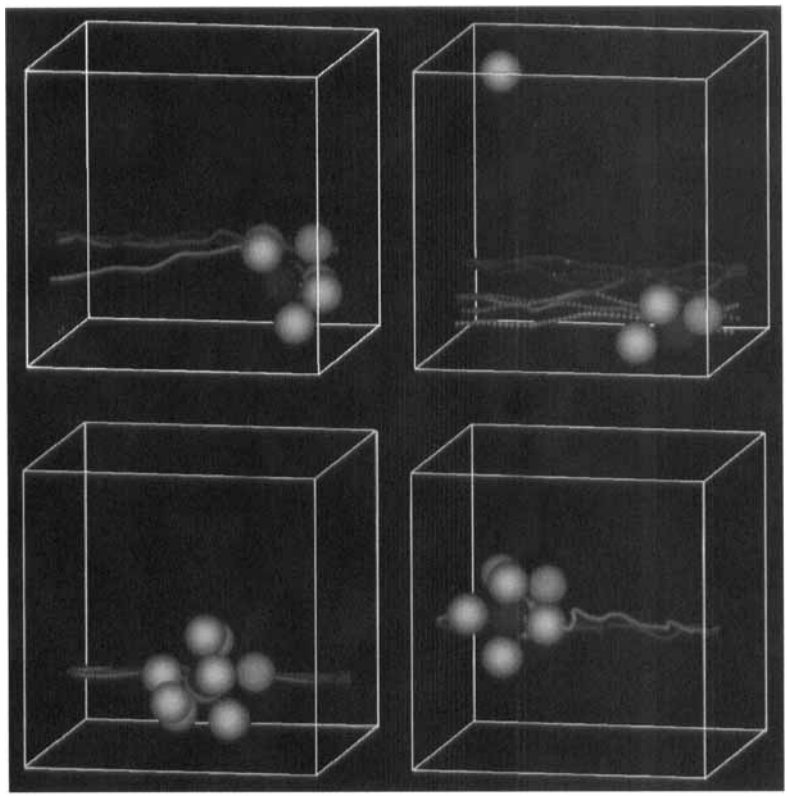

FIGURE 8 Evolution of the trajectory of a selected atom and the configuration of its' local environment at time steps 20250, 20500, 20750 and 21,000 at a reduced shear rate $\dot{\gamma}^* = 3$. See Color Plate VII.

the top half of the figure are moving from right to left and those in the bottom half from left to right. The diameter of the atoms not in the foremost plane have been reduced by a factor of 0.65 to clarify the patterns. One can notice that the atoms are arranged in a stringlike pattern. The absence of atoms between the strings indicates alignment of the strings throughout the entire domain. Rotating the view 90° provides a view of the *y-z* planes, Figure 10, with the foremost plane of atoms exiting the box in the top half and entering the box in the bottom half. This confirms the three dimensional alignment of the strings. In the out-of-shear plane, the *y-z* plane, the atoms are arranged in rows that are rotated from the horizontal. Structural distortions are not surprising at the lower reduced shear rates since the

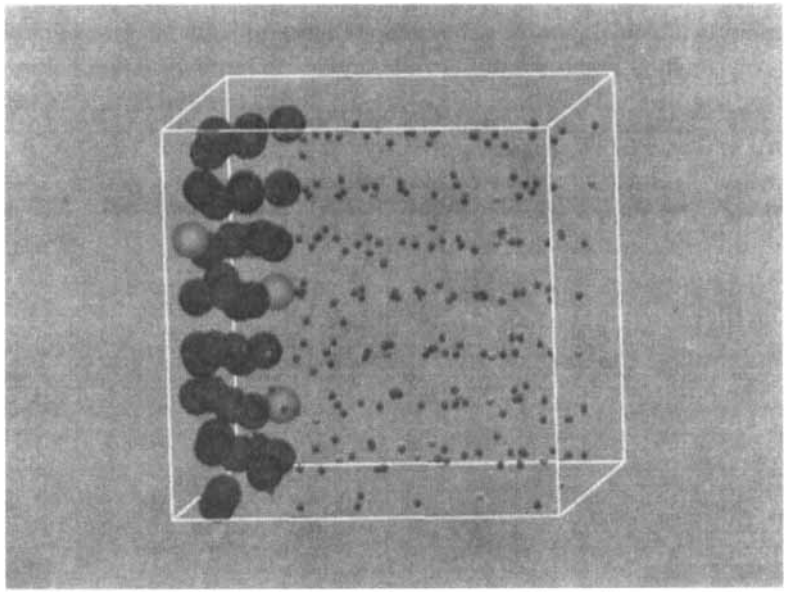

FIGURE 9 Longitudinal alignment of atoms moving in a shear field. The atoms in the top half of the cell are moving from right to left and those in the bottom half are moving from the left to the right. The red atoms are impurity atoms and the green are those of the host liquid. The reduced shear rate is $\dot{\gamma}^* = 3$. See Color Plate VIII.

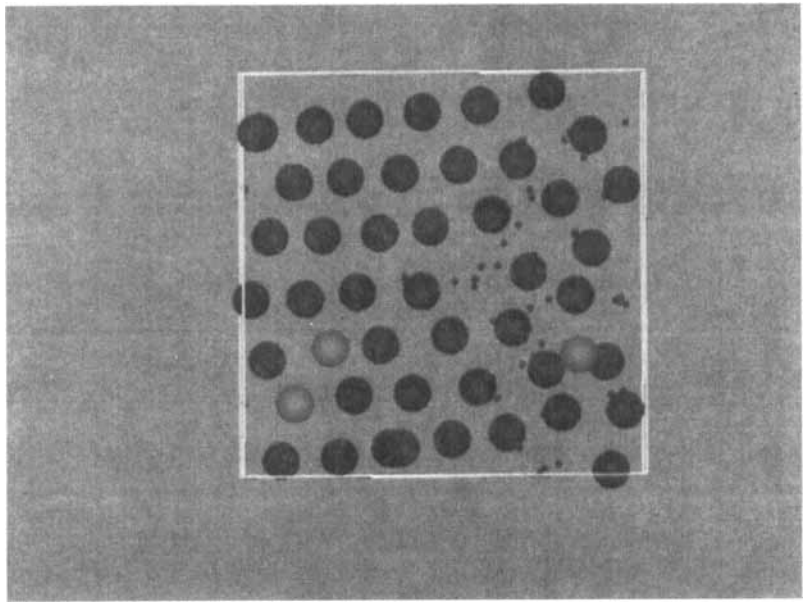

FIGURE 10 View of atom arrangement in the plane normal to the direction of motion. Atoms in the top half are exiting the cell while those in the bottom half are entering the cell. The reduced shear rate is $\dot{\gamma}^* = 3$. See Color Plate IX.

external field has broken the equilibrium symmetry. The onset of ordered structure at the highest shear rate is also in agreement with results of earlier investigators, for example those of Weider *et al.* [8], for systems for both hard and soft spheres.

4. SUMMARY

A set of three-dimensional visualization modules has been developed and incorporated into an existing animation environment to observe the time evolution of local atomic trajectories and local structural ordering in NEMD shear flow simulations. The visualizations have provided not only static snapshots of the non-spherical local environments occurring at all shear rates but also the corresponding time histories of the path of a selected atom within a changing and deforming environment. The visualization capability allows one to examine both the ordered three-dimensional arrangement of atoms occurring at the high shear rates and also the details of the changing local dynamics associated with that ordering which might not otherwise be discerned from static structure factors or small angle neutron scattering data.

Acknowledgements

The authors acknowledge the support of the Office of Naval Research. Computational resources were provided by the Naval Research Laboratory.

References

[1] Heyes, D. H. (1983). *J. Chem. Soc. Fard. Trans. 2*, **79**, 1741.
[2] Sandberg, W. C. and Heyes, D. H. (1995). *Molecular Physics*, **85**, 635.
[3] Evans, D. J. and Morris, G. P. (1984). *Phys. Rev. A*, **30**, 1528.
[4] Hammonds, K. D. and Heyes, D. M. (1988). *J. Chem. Soc. Farad. Trans. 2*, **84**, 705.
[5] Lees, A. W. and Edwards, S. F. (1972). *J.*, **5**, 1921
[6] Obeysekare, U. and Sandberg, W.C. (1995). *AVS Network News*, **2**, 25.
[7] Obeysekare, U., Williams, C., Durbin, J., Rosenblum, L., Rosenberg, R., Grinstein, F., Ramamurti, R., Landsberg, A. and Sandberg, W.C. (1996). *Proc. Visualization'96*, **85**, 635.
[8] Weider, T., Stottut, U., Loose, W. and Hess, S. (1991). *Physica A*, **174**, 1.